Enhanced levels of atmospheric low-molecular weight monocarboxylic acids in gas and particulates over Mt. Tai, North China, during field burning of agricultural wastes

Tomoki Mochizuki[1,2], Kimitaka Kawamura[1,3*], Shinnosuke Nakamura[1,4], Yugo Kanaya[5], and Zifa Wang[6]

[1]Institute of Low Temperature Science, Hokkaido University, Sapporo, Japan
[2]Now at School of Food and Nutritional Sciences, University of Shizuoka, Shizuoka, Japan
[3]Now at Chubu Institute for Advanced Studies, Chubu University, Kasugai, Japan
[4]Graduate School of Environmental Science, Hokkaido University, Sapporo, Japan
[5]Research Institute for Global Change, Japan Agency for Marine-Earth Science and Technology, Yokohama, Japan
[6]LAPC, Institute of Atmospheric Physics, Chinese Academy of Sciences, Beijing, China

*Correspondence: kkawamura@isc.chubu.ac.jp

Published in Atmospheric Environment

Highlights:

We determined gaseous and particulate C_1-C_{10} monocarboxylic acids over Mt. Tai.

Formic (C_1) and acetic (C_2) acids were dominant followed by lactic acid.

High concentrations of C_1 and C_2 were observed during field burning of wheat straw.

High particle-phase fractions of C_1 (0.50) and C_2 (0.31) were observed.

Field burning of agricultural wastes is an important source of monocarboxylic acids.

Keywords: Acetic acid, Formic acid, Lactic acid, Gas/particle partitioning, Wheat straw burning, North East China

Abstract

To understand the source and atmospheric behaviour of low molecular weight monocarboxylic acids (monoacids), gaseous (G) and particulate (P) organic acids were collected at the summit of Mt. Tai in the North China Plain (NCP) during field burning of agricultural waste (wheat straw). Particulate organic acids were collected with neutral quartz filter whereas gaseous organic acids were collected with KOH-impregnated quartz filter. Normal (C_1-C_{10}), branched (iC_4-iC_6), hydroxy (lactic and glycolic), and aromatic (benzoic) monoacids were determined with a capillary gas chromatography employing *p*-bromophenacyl esters. We found acetic acid as the most abundant gas-phase species whereas formic acid is the dominant particle-phase species. Concentrations of formic (G/P 1570/1410 ng m^{-3}) and acetic (3960/1120 ng m^{-3}) acids significantly increased during the enhanced field burning of agricultural wastes. Concentrations of formic and acetic acids in daytime were found to increase in both G and P phases with those of K^+, a field-burning tracer (r = 0.32–0.64). Primary emission and secondary formation of acetic acid is linked with field burning of agricultural wastes. In addition, we found that particle-phase fractions (F_p =P/(G+P)) of formic (0.50) and acetic (0.31) acids are significantly high, indicating that semi-volatile organic acids largely exist as particles. Field burning of agricultural wastes may play an important role in the formation of particulate monoacids in the NCP. High levels (917 ng m^{-3}) of particle-phase lactic acid, which is characteristic of microorganisms, suggest that microbial activity associated with terrestrial ecosystem significantly contributes to the formation of organic aerosols.

1. Introduction

Low molecular weight (LMW) monocarboxylic acids (monoacids) are known to exist in the atmosphere as gases, aerosols, cloud, fog, and snow (Kawamura et al., 1985; Chebbi and Carlier, 1996; Kawamura et al., 2012). Formic and acetic acids are dominant organic species in the atmosphere. Concentrations of formic and acetic acids in gas phase are higher than those in particle phase (e.g., Andreae et al., 1988, Liu et al., 2012) due to their high vapour pressures. Global gaseous formic acid emission is estimated to be 100-120 Tg $year^{-1}$ (Stavrakou et al., 2011), where formic acid comprises about 10% of the total emissions of non-methane volatile organic compounds. However, there is a significant missing source of organic acids. In particular, there is a limitation on our knowledge on how LMW monoacids exist in particles and what parameters control the gas/particle portioning of those organic acids.

Particulate formic and acetic acids are water-soluble and thus play an important role in the balance of radiative forcing acting as cloud condensation nuclei (CCN) (Yu, 2000). Gaseous formic and acetic acids are adsorbed on the existing alkaline particles. Möhler et al. (2008) reported that ice nuclei (IN) efficiency of mineral dust particles is decreased by the adsorptive uptake of organics on the particle surface. However, effects of organics on CCN and IN largely depend on their chemical composition or polarity. The organic aerosols that are enriched with organic acids contribute to the formation of CCN and IN and thus precipitation process, affecting the global water cycle and climate changes. On the other hand, high abundances of LMW organic acids in the atmosphere can adversely affect air quality and human health and also increase the acidity of rainwater (Keene et al., 1983, 1989; Kawamura et al., 1996).

Previous studies have shown that LMW monoacids are derived from both primary and secondary sources. LMW monoacids are directly emitted from fossil fuel combustion (Kawamura et al., 2000), vegetation (Kesselmeier and Staudt, 1999), soils (Asensio et al.,

2008), and ocean microorganisms (Miyazaki et al., 2014). The secondary sources include photooxidation of biogenic and anthropogenic organic compounds (Kawamura et al., 2000; Lim et al., 2005; Paulot et al., 2011; Brégonzio-Rozier et al., 2015). In addition, biomass burning is an important source of formic and acetic acids in gas and aerosol phases (Andreae et al., 1988; Kesselmeier and Staudt, 1999). However, gas/particle partitioning of formic and acetic acids emitted from biomass burning has rarely been studied. Further, there is no study on gas/particle partitioning of normal (C_3–C_{10}), branched chain (iC_4–iC_6), and hydroxy (lactic acid) monoacids in the atmosphere.

East China is one of the most polluted regions in the world, where many mega cities such as Beijing and Shanghai are located. Our previous studies reported that concentrations of levoglucosan, a biomass burning tracer (Fu et al., 2008), dicarboxylic acids (Kawamura et al., 2013a), and α-dicarbonyls (Kawamura et al., 2013b) significantly increased over the summit of Mt. Tai in the North China Plain (NCP) during the field burning of agricultural wastes. The inflow of those polluted air masses may adversely affect the air quality even in urban areas such as Beijing and outflow regions in East Asia and the western North Pacific.

In this study, we collected gas and particle samples at the summit of Mt. Tai during June 2006 to better understand the distributions of LMW monoacids during the field burning of agricultural residue. We utilized two-stage filter pack sampling technique (see the experimental section) followed by derivatization to *p*-bromophenacyl esters to determine gas and particulate monoacids simultaneously (Kawamura et al., 1985). Further, utilization of a capillary gas chromatograph (GC) provides very high resolution and sensitivity and hence relatively minor species such as propionic acid (C_3) and C_4-C_{10} monoacids, which are not detectable by ion chromatography, can be detected by GC method (Kawamura et al., 1985). By modifying the method of Kawamura et al. (1985), we determined hydroxy (lactic and glycolic) acids together with normal (C_1–C_{10}), branched (iC_4–iC_6), and aromatic (benzoic) monoacids in both gas and aerosol phases. Although this technique has been used for air and

rainwater samples from Los Angeles (Kawamura et al., 2000, 2001), it application has not been conducted to air samples from Asian regions. Here we report, for the first time, gaseous and particulate LMW monoacids that are most likely derived from the field burning of agricultural wastes. We also discuss gas/particle partitioning of monoacids during the field burning of wheat straws in the NCP and potential contribution of microbial activity to organic aerosols.

2. Experimental

Sampling of gaseous and particulate LMW monoacids was conducted at the top of Mt. Tai (36.26º N, 117.11º E, elevation: 1534 m above sea level) located in Shandong Province, North China (Figure 1) as part of the Mount Tai Experiment 2006 campaign (MXT2006) (Kanaya et al., 2013). Sample collections were performed every 3 hours (00:00–03:00, 03:00–06:00, 06:00–09:00, 09:00–12:00, 12:00–15:00, 15:00–18:00, 18:00–21:00, 21:00–24:00 LT) on June 2–5 and 23–25, 2006. Totally 36 sets of samples (72 filters) were collected for both particulate and gaseous LMW monoacids employing neutral and KOH-impregnated quartz fibre filters, respectively. Here, we compare the atmospheric abundances of gaseous and particulate organic acids between more and less field-burning periods. The weather conditions were sunny or cloudy during the campaign. Meteorological parameters such as ambient temperature, relative humidity, wind direction, and wind speed were measured at the Mt. Tai Observatory and reported previously (Kanaya et al., 2013; Kawamura et al., 2013a). The height of planetary boundary layer (PBL) are provided by the Global Data Assimilation System (GDAS1) (Air Resources Laboratory, NOAA). Average PBL in daytime and nighttime were about 2200 m and about 600 m, respectively. Daytime samples were collected within the PBL and nighttime samples were collected in the free troposphere during the sampling period.

To collect ambient monoacids in gas and particle phases, a low-volume air sampler

126 equipped with the two-stage filter packs (URG-2000-30FG) were set in a series at the
127 balcony of two-story building of the observatory (height: 10 m) near the summit of Mt. Tai.
128 Total particulate monoacids were collected on precombusted (450 °C, 6 h) neutral
129 quartz-fiber filter (47 mm diameter) (first stage) whereas gaseous monoacids were collected
130 on the quartz-fiber filter impregnated with potassium hydroxide (KOH) (second stage) at an
131 airflow rate of 8.4 L min^{-1}. The KOH impregnated filters were prepared by rinsing the
132 precombusted quartz filter in a 0.2 M KOH solution and then dried in an oven at 80 °C. The
133 details of filter preparation and analytical method were described previously (Kawamura et
134 al., 1985). Both the neutral and alkaline filters were individually placed in clean glass vials
135 (50 ml) with a Teflon-lined screw cap to avoid a gas exchange with ambient air before and
136 after the sampling. After the sampling, filter samples were transported to the lab in Sapporo
137 and stored in a freezer room at -20 °C prior to analysis.

138 An aliquot of filter (4.3 cm^2) was extracted with organic free ultrapure water (5 ml ×
139 3, > 18.2 MΩ cm) under ultrasonication. To remove particles and filter debris, the extracts
140 were passed through a Pasteur pipette packed with quartz wool. To avoid the evaporative loss
141 of volatile monoacids during analytical procedures, the pH of water extracts was adjusted to
142 8.5-9.0 with 0.05 M KOH solution to form organic acid salts (e.g., $CH_3COO^-K^+$). The organic
143 acid salts were concentrated using a rotary evaporator under vacuum at 50 °C. To make all
144 the organic acid salts to $RCOO^-K^+$ form, the concentrates were passed through a cation
145 exchange resin (DOWEX 50W-X4, 100-200 mesh, K^+ form) packed in a Pasteur pipette. The
146 eluents were finally checked for pH=8.5–9.0 and then concentrated using a rotary evaporator
147 under vacuum. The dried $RCOO^-K^+$ salts were derivatized in acetonitrile (4 ml) with
148 α,*p*-dibromoacetophenone (0.1 M, 50 μl) as a derivatization reagent and
149 dicyclohexyl-18-crown-6 (0.01 M, 50 μl) as a catalyst at 80 °C for 2 hours (Kawamura and
150 Kaplan, 1984).

151 The derivatives (*p*-bromophenacyl esters) of monoacids including normal (C_1–C_{10}),

152 branched (iC_4–iC_6), and aromatic (benzoic acid) structures were measured using a capillary
153 gas chromatograph (GC) (HP GC6890, Hewlett-Packard, USA) equipped with a flame
154 ionization detector. The GC peaks were identified using a GC-mass spectrometer (GC/MS)
155 (Agilent GC7890A and 5975C MSD, Agilent, USA). The mass spectra of *p*-bromophenacyl
156 esters of monoacids are presented in Kawamura and Kaplan (1984).

157 The OH functional groups in *p*-bromophenacyl esters of organic acids were further
158 reacted with N,O-bis-(trimethylsilyl)trifluoroacetamide (BSTFA) with 1% trimethylsilyl
159 chloride and 10 μl of pyridine at 70 °C for 3 hours to derive trimethylsilyl (TMS) ethers of
160 *p*-bromophenacyl esters. The derived TMS ethers were determined with a capillary GC and
161 GC/MS. We determined hydroxymonocarboxylic acids including lactic and glycolic acids.
162 Details of the methods have been described in Kawamura et al. (2012).

163 A mixture of organic acids was prepared in our laboratory from the authentic
164 standards: C_1-C_7 and iC_4-iC_6 (10 mM in water, assay 98%, Sigma-Aldrich), lactic acid (assay
165 >85%, Wako), glycolic acid (assay 97%, Wako), and benzoic acid (assay 99%, Tokyo
166 Chemical Industry Co.). To check the recoveries of organic acids during the analytical
167 procedures, authentic monoacid standards (C_1–C_{10}, benzoic, lactic, and glycolic acids) were
168 spiked to KOH-impregnated quartz filters and the filters were analysed as a real sample. The
169 results showed that the recoveries were more than 80%. Analytical errors using authentic
170 standards were within 12%. Detection limits of organic acids in our analytical method were
171 ca. 0.02 ng m^{-3}. Filed blank filters were prepared by the same sampling procedures without
172 pumping air. We found that blank levels of monoacids were less than ~5% of those of
173 ambient samples in both gaseous and particulate phases. In addition, we analyzed laboratory
174 blanks for monoacids, in which the same analytical protocols were used. The blank levels
175 were less than ~5% of those of ambient samples. The concentrations reported here are
176 corrected against the field and laboratory blanks, but not corrected for the recoveries.

177 Particulate organic acids collected on the neutral filter may be in part evaporated

178 during sampling and be collected on the second filter (KOH-impregnated). Thus, particulate
179 organic acids could be underestimated and gaseous organic acids could be overestimated.
180 However, we believe that evaporative loss should be minimal based on the experimental
181 results from Los Angeles (Kawamura et al., 1985, 2000). Samplings of total suspended
182 particles over the Mt. Tai and Los Angeles were conducted by the same sampling system.
183 Particle phase (TSP) concentrations of organic acids from Mt. Tai (C_1: 1410 ng m^{-3}, C_2: 1120
184 ng m^{-3}) are higher than those (C_1: 163 ng m^{-3}, C_2: 120 ng m^{-3}) from Los Angeles (Kawamura
185 et al., 2000). Particulate organic acids collected on a neutral quartz filter (first stage) have
186 been reported to be less than ~17% of total (gas + particulate) organic acids in Los Angeles
187 (Kawamura et al., 1985). We found that particulate monoacids are sometimes more abundant
188 than gaseous monoacids in this study, which may be in part associated with lower ambient air
189 temperature on the top of Mt. Tai (12-20 °C, average 16°C) than in Los Angeles (summer)
190 and other parameters as discussed later.

191 Keene et al. (1989) showed that alkaline (NaOH) impregnated filter with glycerol
192 ($C_3H_8O_3$) results in positive interferences of formic and acetic acids. Concentrations of formic
193 and acetic acids in gas phase may be overestimated in the previous studies where glycerol
194 was used because glycerol may be reacted with oxidants to result in formic and acetic acids.
195 However, we did not use glycerol in this study. Gaseous monoacids may be subjected to
196 atmospheric titration by alkaline dust particles (Ca, Na, K and Mg) in the atmosphere.
197 Organic acids in aerosols may exist in the form of salts such as RCOOK, RCOONa, and
198 others. Vapor pressures of those salts are significantly lower than those of free monoacids. In
199 this study, aerosol samples were collected to differentiate free organic acids and organic acid
200 salts using KOH-impregnated and neutral quartz filters, respectively. We calculated ion
201 balance in the aerosols over Mt. Tai (Please see discussion section). Total cations are slightly
202 higher than total anions. We think that absorption of gas phase organic acids in aerosol phase
203 on the first filter is limited.

For the measurements of inorganic ions (cations: Na^+, NH_4^+, K^+, Mg^{2+}, and Ca^{2+} and anions: F^-, MSA^-, Cl^-, NO_2^-, NO_3^-, Br^-, PO_4^{3-}, and SO_4^{2-}), ambient aerosols were collected onto quartz-fiber filter (20 × 25 cm) (Tissuquartz 2500QAT-UP, Pallflex, USA) using a high-volume air sampler during the same sampling period. A portion of filter was extracted with ultrapure water under ultrasonication. The water extracts were filtered through a membrane disk filter (0.22 μm, Millipore Millex-GV, Merck, USA) and then analyzed using an ion chromatograph (Model 761 compact IC, Metrohm, Switzerland) (Miyazaki et al., 2009). Anion analysis was conducted using a Shodex SI-90 4E column and a 1.8 mM Na_2CO_3 + 1.7 mM $NaHCO_3$ solution as an eluent. Cation analysis was performed using a C2-150 column and a 4.0 mM tartaric acid plus 1.0 mM dipicolinic acid solution as an eluent. The analytical errors in duplicate analyses of samples were within 4%.

Carbon monoxide (CO) concentration was continuously monitored with a non dispersive infrared gas analyzer (Model 48C, Thermo Scientific, USA). The CO data were obtained from Kanaya et al. (2009).

Seven-day backward and forward air mass trajectories were calculated over the summit of Mt. Tai at a level of 1500 m and 750 m a.s.l. using the Meteorological Data Explorer (METEX) from the National Institute for Environmental Studies, Tsukuba, Japan (http://db.cger.nies.go.jp/metex/index.html). Meteorological data were obtained from the National Centers for Environmental Prediction (NCEP) Reanalysis data. In addition, we have checked weather conditions in Mt. Tai, Beijing, and Shanghai. Weather information were obtained from the National Oceanic and Atmospheric Administration. Extreme weather events did not occur during the period 28 May to 30 June 2006. Fire spot data sets were downloaded from MODIS fire spot measurement data (http://earthdata.nasa.gov/data/near-real-time-data/firms).

3. Results

230 **3.1. Characteristics of air mass and fire spots**

231 Figure 2 shows typical ten-day air mass back trajectories (1500 m a.s.l.) with fire
232 spots. In the North China Plain (NCP), harvest season of wheat starts in late May and then
233 agricultural wastes (wheat straw) are burned in the open field. The field burning was heavily
234 observed from the satellite over the NCP from 2 to 4 June, especially, in the south of Mt. Tai.
235 The field burning declined during 23–25 June with a shift of the hot spot areas to the north
236 and northwest of the sampling site. The air masses at a levels of 1500 m and 750 m (Please
237 see Figure A1) during 3–4 June have passed over the heavy fire spot regions. These days are
238 strongly influenced by the agricultural waste burning. On the other hand, the air mass (1500
239 m and 750 m) of 2 June was mainly originated from the Sea of Japan. The air masses at a
240 level of 1500 m on 23 and 25 June were transported from the NCP and South China,
241 respectively. Although the air masses at a level of 1500 m on 23 and 25 June were not
242 consistent with those of 750 m, the air masses of 2, 23 and 25 June were less affected by the
243 field burning of agricultural wastes. In addition, concentrations of K^+, a good tracer of field
244 burning (Andreae, 1983), increased on 3–5 June and decreased on 23 and 25 June (Figure 3).
245 These results are consistent with the spatial distributions of fire spots and air mass trajectories
246 arriving over the sampling site. Hence, the air masses of 3–4 June were primarily delivered
247 from the areas of the field burning of agricultural residue. In this study, the data were
248 categorized into two periods: more field-burning (MFB) (3–5 June) and less field-burning
249 (LFB) (2 and 23–25 June) influenced periods.

250

251 **3.2. Gaseous and particulate LMW monoacids**

252 We identified LMW monoacids; such as normal (formic: C_1, acetic: C_2, propionic:
253 C_3, butyric: C_4, pentanoic: C_5, hexanoic: C_6, heptanoic: C_7, octanoic: C_8, nonanoic: C_9, and
254 decanoic: C_{10}), branched chain (isobutyric: iC_4, isopentanoic: iC_5, and isohexanoic: iC_6),
255 hydroxy acids (lactic: Lac, and glycolic: Glyco), and aromatic (benzoic: Benz) acids in both

gas and particle phases. Figure 4 shows average molecular compositions of detected LMW monoacids in the MFB and LFB periods. Acetic acid was the dominant species in gas phase in the MFB (61%) and LFB (41%) periods, followed by formic acid (MFB: 24%, LFB: 29%) and lactic acid (MFB: 5%, LFB: 14%). In particle phase, formic acid was the dominant species in the MFB (34%) and LFB (31%) periods, followed by acetic acid (MFB: 27%, LFB: 27%) and lactic acid (MFB: 22%, LFB: 23%). In addition, isopentanoic acid in particle phase was the fourth most abundant monoacid in the MFB (8%) and LFB (7%) periods. Nonanoic acid (C_9) is the fifth most abundant monoacid in both gas- and particle-phases, showing a peak in the range of C_5-C_{10} monoacids during the MFB and LFB periods (Table 1). C_9 is an oxidation product of oleic acid ($C_{18:1}$) containing a double bond at C-9 position (Kawamura and Gagosian, 1987).

Figure 3 shows temporal variations in the concentrations of major LMW monoacids in gas and particle phases. The gaseous concentrations of acetic acid during the MFB period (3–5 June) are significantly higher than those during the LFB period (2 and 23–25 June). Similarly, the gas-phase concentrations of formic acid are higher during the MFB period than the LFB period. The particle-phase concentrations of formic and acetic acids during the MFB period are slightly higher than those during the LFB period. We found that particle-phase formic and acetic acids were less abundant in the morning and nighttime hours but maximized around noontime or in the afternoon. Two peaks of isopentanoic (iC_5) and lactic (Lac) acids in particle-phase were observed at 6:00–9:00 on 3 June and 9:00–12:00 on 4 June when the field burning of agricultural wastes increased (Figure 2a). However, these acids did not show any diurnal trend in both gas and particle phases.

Concentrations of total monoacids in gas-phase ranged from 1530 to 12,100 ng m^{-3} whereas those in particle-phase ranged from 960 to 9680 ng m^{-3}. Mean concentrations of total monocarboxylic acids in gas-phase were 6540 ng m^{-3} during the MFB and 3070 ng m^{-3} during the LFB period, whereas those in particle-phase were 4120 ng m^{-3} during the MFB

and 2850 ng m^{-3} during the LFB period. Overall, gas-phase concentrations of total monoacids are higher than those of particle phase in both MFB and LFB periods. Table 1 summarises average concentrations of individual monoacids over Mt. Tai. In gas-phase, acetic acid was found as the dominant monoacid species (MFB: 3960 ng m^{-3}, LFB: 1270 ng m^{-3}) followed by formic acid (MFB: 1570 ng m^{-3}, LFB: 890 ng m^{-3}) and lactic acid (MFB: 319 ng m^{-3}, LFB: 433 ng m^{-3}). In particle-phase, formic acid is the dominant species (MFB: 1410 ng m^{-3}, LFB: 883 ng m^{-3}) followed by acetic acid (MFB: 1120 ng m^{-3}, LFB: 763 ng m^{-3}), and lactic acid (MFB: 917 ng m^{-3}, LFB: 661 ng m^{-3}). Mean concentrations of major monoacids in both gas and particle phases are greater during the MFB period than the LFB period, except for gaseous lactic acid and isopentanoic acid (iC_5).

The particle-phase fractions (F_p) of each organic acid were calculated as $F_p = P/(G+P)$, where P is the particle-phase concentration and G is the gas phase concentration. Figure 5 shows temporal variations in the F_p of major monoacids. F_p of acetic (C_2) and propionic (C_3) acids are slightly lower during the MFB period (3–5 June) than other period. The F_p for other LMW monocarboxylic acids over Mt. Tai did not show any clear temporal or diurnal variations. Table 1 also summarizes mean F_p for individual monoacids during the MFB and LFB periods. F_p of individual monoacids during the MFB and LFB periods ranged from 0.19 (C_3) to 0.78 (C_6) and 0.27 (C_4) to 0.93 (iC_6), respectively. F_p of acetic acid was 0.24 during the MFB and 0.38 during the LFB, whereas F_p of formic acid was 0.47 during the MFB and 0.52 during the LFB. F_p of acetic and formic acids during the MFB period are significantly lower than those during the LFB period. On the other hand, F_p of hydroxymonoacids, e.g., lactic acid, and branched chain monoacids, e.g., isopentanoic acid, are significantly high (0.62–0.92), however, there is no systematic trend of the F_p values between the MFB and LFB periods (Table 1).

4. Discussion

4.1. Impact of field burning on the concentrations of formic and acetic acids

To evaluate the effect of biomass burning of agricultural wastes on gaseous and particulate formic and acetic acids, we plotted formic and acetic acids against levoglucosan (a good tracer of biomass burning) (Simoneit, 2002) (Figure 6 and Figure A3). Particulate formic and acetic acids in daytime show a weak correlation with levoglucosan during the MFB (C_1: r = 0.29, C_2: r = 0.28) and LFB (C_1: r = 0.28, C_2: r = 0.24) periods. Gaseous formic and acetic acids in daytime did not show a positive correlation with levoglucosan (r = -0.62 – 0.35). In addition, K^+ is emitted from field burning and agricultural activities, which is an open field burning tracer. We plotted formic and acetic acids against K^+ (Figure 7 and Figure A4). Particulate formic and acetic acids in daytime showed a positive correlation with K^+ during the MFB (C_1: r = 0.59, C_2: r = 0.64) and LFB (C_1: r = 0.44, C_2: r = 0.63) periods, whereas particulate formic and acetic acids in nighttime did not show any correlations with K^+ (r = -0.29 – 0.04).

We found that concentrations of gaseous acetic acid in daytime increased with K^+ during the MFB (r = 0.63) and LFB (r = 0.63) periods. Gaseous acetic acid in nighttime showed a positive correlation with K^+ (MFB: r = 0.54, LFB: r = 0.39). However, formic acid in both gas and particle phases in nighttime showed no correlation with K^+ during the MFB and LFB periods (r = -0.29 – 0.38). We found that particulate formic and acetic acids and gaseous acetic acid showed good correlations with K^+ and no correlations with levoglucosan. Our results suggest that particulate formic and acetic acids and gaseous acetic acid are influenced by the open filed burning in the NCP. Although the sampling was conducted in the MFB and LFB periods at this study, the obtained data must be interpreted with caution because of a limited number of samples.

During the sampling periods, concentrations of formic and acetic acids and K^+ in daytime were higher than those in nighttime. Because the top of Mt. Tai in daytime is below the PBL, organic acids as well as other gaseous and aerosols are uplifted to Mt. Tai from the

lowland agricultural areas in the NCP where field burning of wheat straws is widely operated.

Table 2 compares the concentrations of formic and acetic acids in gas- and particle-phases from multiple sites in the world. Particle-phase concentrations of formic (1410 ng m^{-3}) and acetic (1120 ng m^{-3}) acids over Mt. Tai during the MFB period are significantly higher than those reported in Los Angeles (Kawamura et al., 2000), megacities of China such as Beijing (Wang et al., 2005) and Shanghai (Wang et al., 2006), Amazon forest (Andreae et al., 1988) and Taiwan forest (Tsai and Kuo, 2013), and Alaska (Li and Winchester, 1989). On the other hand, the gaseous levels of formic (1570 ng m^{-3}) and acetic (3960 ng m^{-3}) acids over Mt. Tai during the MFB period are lower than those reported in tropical forests from Amazon (Andreae et al., 1988), biomass burning plumes from the Yangtze River Delta region, China (Kudo et al., 2014), urban air from Pasadena (Yuan et al., 2015), and oil and gas fields from Utah (Yuan et al., 2015). The concentrations of formic and acetic acids at Mt. Tai are 2–5 times higher than those reported from Los Angeles (Kawamura et al., 2000), Greenland (Dibb and Arsenault, 2002), and the French Alps (Preunkert et al., 2007), and 1–2 orders of magnitude higher than those reported from the Pacific Ocean (Miyazaki et al., 2014) and Antarctica (Legrand et al., 2012). These comparisons demonstrate that concentrations of formic and acetic acids in gas and particle phases during field burning of wheat straw are relatively high compared with those from other sites.

Carbon monoxide (CO) is originated from biomass burning (Wang et al., 2002) and anthropogenic sources such as fossil fuel combustion. Average concentrations of CO in the MFB and LFB periods were 553 ppb and 467 ppb, respectively (Kanaya et al., 2009), which levels were very high and the air over Mt. Tai during the sampling periods was highly polluted. Mean concentrations of total monoacids in both gas and particle phases are greater during the MFB period (P: 4130 ng m^{-3}, G: 6540 ng m^{-3}) than the LFB period (P: 3070 ng m^{-3}, G: 2860 ng m^{-3}). Field burning of agricultural wastes is an important source of monoacids in

the atmosphere over Mt. Tai. In addition, Figure A2 shows seven-day air mass forward trajectories during the MFB period. The dominant air mass flow at a levels of 1500 m and 750 m was northeasterly and easterly, indicating outflow of air masses to East Asia and the western North Pacific. We suggest that high abundances of monoacids in the particle phases not only degrade the air quality in East Asia but also largely contribute to enhance the hygroscopic properties of ambient aerosols because they are highly water-soluble. A possible formation of gaseous and particulate acetic acid will be discussed in section 4.3.

4.2. Gas/particle partitioning of formic, acetic, and lactic acids

Generally, F_p increases with an increase of carbon numbers of monoacids (Yatavelli et al., 2014). However, the F_p values of formic (0.47–0.52) and acetic (0.24–0.38) acids at the top of Mt. Tai are larger than the values expected from the high vapour pressures of formic ($V_p = 5.6\times10^{-2}$ atm) and acetic ($V_p = 2.1\times10^{-2}$ atm) acids. In addition, F_p values of C_1 and C_2 over Mt. Tai are significantly larger than those reported from the Pacific Ocean (C_1: $F_p = 0.04$, C_2: $F_p = 0.06$) (Miyazaki et al., 2014) and urban Los Angeles (C_1: $F_p = 0.16$, C_2: $F_p = 0.06$) (Kawamura et al., 2000), in which the same sampling and analytical protocols were used. On the other hand, the F_p of lactic acid (0.61 – 0.69) over Mt. Tai is slightly lower than that reported from the Pacific Ocean (0.76 – 0.82) (Miyazaki et al., 2014).

Khan et al. (1995) reported that ambient temperature and relative humidity (RH) are important factors to determine the gas-particle partitioning of organic acids. Gas-particle partitioning of organic acids depend on temperature (related to Henry's law) and RH (related to aerosol liquid water content indicator). In this study, diurnal variations of temperature and RH were observed. However, there is no consistent relationship between F_p of organic acids and temperature or RH. The ambient temperature and RH did not affect aerosol surface characteristics over Mt. Tai.

As a potential reason of higher F_p values for organic acids, chemical states of those

386 acids in ambient aerosols should be considered. For example, ammonia reacts with gaseous
387 acidic species (e.g., oxalic acid) (Paciga et al., 2014). Gas phase acetic acid can be adsorbed
388 on calcite ($CaCO_3$) that is a major component of mineral dust (Alexander et al., 2015).
389 Because the vapour pressures of organic salts are lower than those of free organic acids, gas
390 to particle conversion of organic acids may be an important factor to control their gas/particle
391 partitioning. However, the F_p of formic and acetic acids did not show correlation with
392 alkaline species such as Na^+, K^+, Ca^{2+}, Mg^{2+}, and NH_4^+ (MFB: $r < -0.12$, LFB: $r < 0.24$). We
393 calculated total cation equivalents (Na^+, NH_4^+, K^+, Mg^{2+}, and Ca^{2+}) and total anion
394 equivalents (F^-, MSA^-, Cl^-, NO_2^-, NO_3^-, Br^-, PO_4^{3-}, and SO_4^{2-}) including normal (C_1-C_{10}),
395 branched chain (iC_4-iC_6), aromatic (benzoic), and hydroxyl (lactic and glycolic) monoacids,
396 although CO_3^- and HCO_3^-, as well as unidentified organic anions, were not considered. The
397 slope of more than unity (1.21) indicates that excess cations exist in the aerosols over Mt. Tai.
398 We calculated total cation equivalents minus total anion equivalents (cations - anions) in the
399 particles from Mt. Tai. F_p of formic (C_1) and acetic (C_2) acids did not show a positive
400 correlation with cation - anions (C_1: $r = -0.36$, C_2: $r = -0.28$). Gas to particle conversion of
401 formic and acetic acids over Mt. Tai was not controlled by the above-mentioned excess
402 alkaline species.

403 *Barsanti et al*. [2009] reported that amines can more easily form organic acid salts
404 compared to ammonia. Unfortunately, we did not measure amines in this study. Amines that
405 are derived from vehicle exhaust and animal husbandry (e.g., Cape et al., 2011) and from
406 biomass burning (Ge et al., 2011) could act as a counterpart for free organic acids and those
407 amine-organic acid reactions may contribute to a new particle formation and condensation
408 growth of particles, enhancing the F_p values in the NCP. We suggest that gas/particle
409 partitioning of formic and acetic acids may be influenced by unidentified factors during
410 atmospheric transport over Mt. Tai, which need further study to be clarified in the future.

411

412 **4.3. Primary and secondary sources of formic and acetic acid**

413 Formic acid (C_1) is largely derived from secondary sources (Khwaja et al., 1995,
414 Pommier et al., 2016), whereas acetic acid (C_2) is largely emitted from primary sources
415 (Kawamura et al., 1985, 2000). The ratio of C_1/C_2 in particle phase is an indicator for primary
416 or secondary source of organic acid aerosol. Talbot et al. (1988) reported that high ratio of
417 C_1/C_2 (> 1) means the dominance of secondary sources, whereas low ratio (< 1) means the
418 dominance of primary sources. In this study, average ratio of C_1/C_2 in daytime in the MFB
419 and LFB periods was 1.3 and 1.2, respectively. C_1/C_2 ratios of Mt. Tai are higher than those
420 reported from urban in China (Shanghai: 0.5) (Wang et al., 2006), tropical rain forest (1.0)
421 (Andreae et al., 1988), and Ocean (0.3) (Miyazaki et al., 2014) and are comparable to those
422 reported from urban Los Angeles (1.4) (Kawamura et al., 2000) and China (Beijing: 1.1)
423 (Wang et al., 2005). High ratio of C_1/C_2 in the aerosols of Mt. Tai indicates that secondary
424 sources are important for the formation of organic acids over the Mt. Tai. Daytime maxima of
425 formic and acetic acids in particle phase (Figure 3) also indicate a secondary source for
426 formic and acetic acids.

427 Kawamura et al. (2013) reported that oxalic acid is the most abundant dicarboxylic
428 acid and largely emitted by the field burning of agricultural wastes in the NCP during the
429 same campaign, but its major sources are photochemical processes (secondary sources).
430 Concentrations of formic and acetic acids in particle phase show positive correlations with
431 concentrations of oxalic acid (C_1: r = 0.63, C_2: r = 0.54).

432 CO is an excellent tracer of primary combustion product. To evaluate the primary
433 and secondary sources of formic and acetic acids during the MFB and LFB periods, we
434 examined the relationship between formic acid or acetic acid and CO as shown in Figure 8.
435 Concentrations of particulate acetic acid in daytime were found to increase linearly with CO
436 during the MFB (r = 0.70) and LFB (r = 0.44) periods. Concentrations of gaseous acetic acid
437 also showed a positive correlation with CO (MFB: r = 0.62, LFB: r = 0.49). Concentrations of

particulate formic acid were found to increase linearly with CO during the MFB ($r = 0.64$). However, concentrations of gaseous formic acid during the MFB and LFB periods and particulate formic acid during the LFB period did not correlate with CO ($r < 0.39$). These correlation analyses suggest that emissions of acetic acid in both particle and gas phases over Mt. Tai are enhanced with an increase in the intensity of biomass burning during the MFB periods.

In addition, the slopes of regression lines drawn for acetic acid in gas- and particle-phases and CO are different between the MFB and LBF periods. In particle-phase, higher ratio of acetic acid/CO (0.003) was obtained during the MFB period, whereas lower ratio (0.001) was obtained during the LFB period. In gas-phase, higher ratio of acetic acid/CO (0.006) was obtained during the MFB period, whereas lower ratio (0.001) was obtained during the LFB period. K^+ as a biomass tracer shows a significant correlation with CO, whereas the slopes of the regression lines for K^+ and CO are different between the MFB and LFB periods (Figure A5). Ratio of K^+/CO (0.007) obtained from the slope of K^+ and CO during the MFB period was lower than that during the LFB period (0.001). SO_4^{2-} as a fossil fuel combustion and industrial emission tracer shows a significant correlation with CO, whereas the slopes of the regression lines for SO_4^{2-} and CO are different between the MFB and LFB periods (Figure A6). Ratio of SO_4^{2-}/CO (0.112) obtained from the slope of SO_4^{2-} and CO during the MFB period was lower than that during the LFB period (0.056). The higher ratios of K^+/CO during the MFB period indicate a strong influence of field burning of agricultural wastes in the NCP. The lower ratios of K^+/CO during the LFB period suggest an influence of contribution of CO from other sources such as fossil fuel combustion in the surroundings of North China. These results again suggest that abundant gas- and particle-phase acetic acid is directly emitted from the field burning of agricultural wastes.

During the campaign, ethane, ethene, propane, and propene (highly volatile hydrocarbons) are emitted from open burning of crop residue in the NCP (Kanaya et al.,

2009), which are important precursors of acetic acid (Warneck, 2005). Concentrations of these hydrocarbons were reported to increase under the influence of biomass burning plumes in the NCP (Kanaya et al., 2009). The daytime peaks of particulate and gaseous acetic acid can be explained by secondary processing via photochemical oxidation of volatile hydrocarbons over Mt. Tai. We plotted the ratios of acetic acid in total monocarboxylic acids (C_2/total MCA) against K^+ (Figure 9). Ratios of C_2 to total MCA in both gas- and particle-phases increased with an increase in CO concentrations during the MFB and LBF periods. In particular, contributions of C_2 to total MCA during the MFB period showed a significant correlation with CO (gas: r = 0.93, particle: r = 0.80). These positive correlations suggest that acetic acid is selectively produced in the atmosphere by the photochemical oxidation of volatile hydrocarbons when organic precursors are transported over the summit of Mt. Tai from the field burning areas in lowland. We consider that primary emission and secondary formation of gas- and particle-phase acetic acid are associated with field burning of agricultural wastes in the NCP.

4.4. High abundances of biogenic monocarboxylic acids

Lactic acid is produced by lactobacillus (Cabredo et al., 2009), which is known to exist in soil (Huysman and Verstraete, 1993) and emitted from plant tissues in agricultural farm (primary origin) (Raja et al., 2008). This organic acid can also be produced by the oxidation of isoprene with ozone (Nguyen et al., 2010) (secondary origin). Gaseous and particulate lactic acid did not correlate ($r < -0.15$) with 2-methyltetrols, good tracers of isoprene-derived secondary organic aerosols (Fu et al., 2012). Isopentanoic acid can be produced by bacteria such as *Bacteroides ruminicola* and *Megasphaera elsdenii* (Allison, 1978). We found a strong positive correlation between lactic and isopentanoic acids in both gas (r = 0.91) and particle (r = 0.93) phases (Figure 10). This result is similar to that obtained for snow pit samples from high mountain site in central Japan, although the snow samples are

490 influenced by the outflow of Asian dust (Mochizuki et al., 2016). We suggest that major
491 portion of lactic and isopentanoic acids were directly derived from the terrestrial ecosystem.
492 Microbial productivity involved with lactic and isopentanoic acids should widely exist in the
493 terrestrial ecosystems in China. Hence, we conclude that these LMW monoacids are mainly
494 derived from microbial sources.

495 Average particle phase concentration of lactic acid (789 ng m^{-3}) is one order of
496 magnitude higher than those in marine aerosol samples from the Pacific (33.1 ng m^{-3})
497 (Miyazaki et al., 2014), pasture samples (22.1 ng m^{-3}) and forest samples (9.2 ng m^{-3}) in
498 Brazil (Graham et al., 2002). In addition, average gas phase concentration of lactic acid (376
499 ng m^{-3}) is significantly higher than that reported in the marine atmosphere from the Pacific
500 Ocean (7.1 ng m^{-3}) (Miyazaki et al., 2014). These results suggest that the NCP is an important
501 source of particulate and gaseous lactic acid in the atmosphere. Furthermore, high
502 abundances of isopentanoic acid (iC_5) in particle phase (average, 250 ng m^{-3}) in the ambient
503 aerosols from Mt. Tai were obtained, which is the same order of magnitude as particulate
504 lactic acid. To our knowledge, this is the first observation on the abundances of branched
505 chain monoacids in atmospheric aerosols. In previous studies, hydroxy monoacids such as
506 lactic acid and branched chain monoacids such as isopentanoic acid are scarcely reported
507 (Kawamura et al., 2012; Miyazaki et al., 2014; Mochizuki et al., 2016) We propose that
508 measurements of biogenic hydroxy and branched chain monoacids are important to evaluate
509 the source of organic aerosols and their atmospheric chemical processing.
510

511 **5. Summary and conclusions**

512 Gaseous (G) and particulate (P) low molecular weight (LMW) monocarboxylic acids,
513 including normal (C_1-C_{10}), branched (iC_4-iC_6), hydroxyl (lactic and glycolic), and aromatic
514 (benzoic) structures, were detected in the ambient air samples collected at the summit of Mt.
515 Tai in the North China Plain (NCP). We found that acetic acid was the most abundant

gaseous species whereas formic acid was the most abundant particulate species. Significantly high concentrations of formic (average, G: 1570 ng m^{-3}, P: 1410 ng m^{-3}) and acetic (G: 3960 ng m^{-3}, P: 1120 ng m^{-3}) acids were detected during the period of inflow of air plumes from the field burning of agricultural waste (wheat straw) in the NCP. Because gas- and particle-phase concentrations of formic and acetic acids in daytime are correlated (r = 0.32–0.64) with K^+ (a field burning tracer), field burning of agricultural waste should be an important primary source of LMW monoacids over Mt. Tai. In addition, we found a large fraction (F_p) of particulate formic (0.49) and acetic (0.32) acids in the total (G+P) concentrations. We suggest that primary emission and secondary formation of gaseous and particulate acetic acid are associated with field burning of agricultural waste in the NCP. We also found high concentrations of isopentanoic acid (331 ng m^{-3}) and lactic acid (917 ng m^{-3}) in particle phase, suggesting that biological sources are also important for LMW monoacids in organic aerosols. LMW monoacids emitted from the field burning of agricultural wastes importantly contribute to the formation of organic aerosols in Central East China.

Acknowledgements

This study was in part supported by the Japanese Ministry of Education, Culture, Sports, Science and Technology (MEXT) through grant-in-aid Nos. 17340166, 1920405 and 24221001. We also acknowledge the financial support by the Global Environment Research Fund (B-051) of the Ministry of the Environment, Japan, for the shipping of the instruments to Mt. Tai. We thank K. Okuzawa and S. G. Aggarwal for their supports during sample collection. We also thank Dr. Pakpong Pochanart for the collection of CO data. The data of this paper are available upon request to K. Kawamura (kkawamura@isc.chubu.ac.jp).

References

541 Alexander, J.M., Grassian, V.H., Young, M.A., Kleiber, P.D., 2015. Optical properties of
542 selected components of mineral dust aerosol processed with organic acids and humic
543 material. J. Geophys. Res. Atmos. 120, 2437-2452, doi:10.1002/2014JD022782.
544 Allison, M.J., 1978. Production of branched-chain volatile fatty-acids by certain anaerobic
545 bacteria. Appl. Environ. Microbiol. 35, 872-877.
546 Andreae, M.O., 1983. Soot carbon and excess fine potassium: long-range transport of
547 combustion-derived aerosols. Science 10, 1148-1151.
548 Andreae, M.O., Talbot, R.W., Andreae, T.W., Harris, R.C., 1988. Formic and acetic acid over
549 the central Amazon region, Brazil. 1. Dry season. J. Geophys. Res. 93, 1616-1624.
550 Asensio, D., Peñuelas, J., Prieto, P., Estiarte, M., Filella, I., Llusià, J., 2008. Interannual and
551 seasonal changes in the soil exchange rates of monoterpenes and other VOCs in a
552 Mediterranean shrubland. Eur. J. Soil Sci. 59, 878-891.
553 Barsanti, K.C., McMurry, P.H., Smith, J.N., 2009. The potential contribution of organic salts
554 to new particle growth. Atmos. Chem. Phys. 9, 2949-2957.
555 Brégonzio-Rozier, L., Siekmann, F., Giorio, C., Pangui, E., Morales, S.B., Temime-Roussel,
556 B., Gratien, A., Michoud, V., Ravier, S., Cazaunau, M., Tapparo, A., Monod, A.,
557 Doussin, J.-F., 2015. Gaseous products and secondary organic aerosol formation during
558 long term oxidation of isoprene and methacrolein. Atmos. Chem. Phys. 15, 2953-2968,
559 doi:10.5194/acp-15-2953-2015.
560 Cabredo, S., Parra, A., Saenz, C., Anzano, J., 2009. Bioaerosols chemometric
561 characterization by laser-induced fluorescence: air sample analysis. Talanta 77,
562 1837-1842.
563 Cape, J.N., Cornell, S.E., Jickells, T.D., Nemitz, E., 2011. Organic nitrogen in the
564 atmosphere – Where does it come from? A review of sources and methods. Atmos. Res.
565 102, 30-48, doi:10.1016/j.atmosres.2011.07.009.

566 Chebbi, A., Carlier, P., 1996. Carboxylic acids in the troposphere, occurrence, sources, and
567 sinks: A review. Atmos. Environ. 30(24), 4233-4249.
568 Dibb, J.E., Arsenault, M., 2002. Shouldn't snowpacks be sources of monocarboxylic acids?
569 Atmos. Environ. 36, 2513-2522.
570 Fu, P.Q., Kawamura, K., Okuzawa, K., Aggarwal, S.G., Wang, G., Kanaya, Y., Wang, Z.,
571 2008. Organic molecular compositions and temporal variations of summertime mountain
572 aerosols over Mt. Tai, North China Plain. J. Geophys. Res. 113, D19107,
573 doi:10.1029/2008JD009900.
574 Fu, P.Q., Kawamura, K., Chen, J., Li, J., Sun, Y.L., Liu, Y., Tachibana, E., Aggarwal, S.G.,
575 Okuzawa, K., Tanimoto, H., Kanaya, Y., Wang, Z.F., 2012. Diurnal variations of organic
576 molecular tracers and stable carbon isotope composition in atmospheric aerosols over Mt.
577 Tai in the North China Plain: an influence of biomass burning. Atmos. Chem. Phys. 12,
578 8359-8375, doi:10.5194/acp-12-8359-2012.
579 Ge, X., Wexler, A.S., Clegg, S.L., 2011. Atmospheric amines – Part I. A review. Atmos.
580 Environ. 45, 524-546.
581 Graham, B., Mayol-Bracero, O.L., Guyon, P., Roberts, G.C., Decesari, S., Facchini, M.C.,
582 Artaxo, P., Maenhaut, W., Köll, P., Andreae, M.O., 2002. Water-soluble organic
583 compounds in biomass burning aerosols over Amazonia 1. Characterization by NMR and
584 GC-MS. J. Geophys. Res. 107(D20), 8047, doi:10.1029/2001JD000336.
585 Huysman, F., Verstraete, W., 1993. Water-facilitated transport of bacteria in unsaturated soil
586 columns: influence of cell surface hydrophobicity and soil properties. Soil Biol. Biochem.
587 25(1), 83-90.
588 Kanaya, Y., Pochanart, P., Liu, Y., Li, J., Tanimoto, H., Kato, S., Suthawaree, J., Inomata, S.,
589 Taketani, F., Okuzawa, K., Kawamura, K., Akimoto, H., Wang, Z.F., 2009. Rates and
590 regimes of photochemical ozone production over Central East China in June 2006: a box

591 model analysis using comprehensive measurements of ozone precursors. Atmos. Chem.
592 Phys. 9, 7711-7723.
593 Kanaya, Y., Akimoto, H., Wang, Z.-F., Pochanart, P., Kawamura, K., Liu, Y., Li, J.,
594 Komazaki, Y., Irie, H., Pan, X.-L., Taketani, F., Yamaji, K., Tanimoto, H., Inomata, S.,
595 Kato, S., Suthawaree, J., Okuzawa, K., Wang, G., Aggarwal, S.G., Fu, P.Q., Wang, Y.,
596 Zhuang, G., 2013. Overview of the Mt. Tai Experiments (MTX2006) in central East
597 China in June 2006: studies of significant regional air pollution. Atmos. Chem. Phys. 13,
598 8265–8283.
599 Kawamura, K., Kaplan, I.R., 1984. Capillary gas chromatography determination of volatile
600 organic acids in rain and fog samples. Anal. Chem. 56, 1616-1620.
601 Kawamura, K., Ng, L.L., Kaplan, I.R., 1985. Determination of organic-acids (C_1-C_{10}) in the
602 atmosphere, motor exhausts, and engine oils. Environ. Sci. Technol. 19, 1082-1086.
603 Kawamura, K., Gagosian, R.B., 1987. Implications of ω-oxocarboxylic acids in the remote
604 marine atmosphere for photo-oxidation of unsaturated fatty acids. Nature 325, 330-332.
605 Kawamura, K., Steinberg, S., Kaplan, I.R., 1996. Concentrations of mono- and di-carboxylic
606 acids and aldehydes in southern California wet precipitations: comparison of urban and
607 non-urban samples and compositional changes during scavenging. Atmos. Environ. 30,
608 1035-1052.
609 Kawamura, K., Steinberg, S., Kaplan, I.R., 2000. Homologous series of C_1-C_{10}
610 monocarboxylic acids and C_1-C_6 carbonyls in Los Angeles and motor vehicle exhausts.
611 Atmos. Environ. 34, 4175-4191.
612 Kawamura, K., Steinberg, S., Ng, L., Kaplan, I.R., 2001. Wet deposition of low molecular
613 weight mono- and di-carboxylic acids, aldehydes and inorganic species in Los Angeles.
614 Atmos. Environ. 35, 3917-3926.
615 Kawamura, K., Matsumoto, K., Tachibana, E., Aoki, K., 2012. Low molecular weight
616 (C_1-C_{10}) monocarboxylic acids, dissolved organic carbon and major inorganic ions in

617 alpine snow pit sequence from a high mountain site, central Japan. Atmos. Environ. 62,
618 272-280.
619 Kawamura, K., Tachibana, E., Okuzawa, K., Aggarwal, S.G., Kanaya, Y., Wang, Z.F., 2013a.
620 High abundances of water-soluble dicarboxylic acids, ketocarboxylic acids and
621 α-dicarbonyls in the mountaintop aerosols over the North China Plain during wheat
622 burning season. Atmos. Chem. Phys. 13, 8285-8302, doi:10.5194/acp-13-8285-2013.
623 Kawamura, K., Okuzawa, K., Aggarwal, S.G., Irie, H., Kanaya, Y., Wang, Z., 2013b.
624 Determination of gaseous and particulate carbonyls (glycolaldehyde, hydroxyacetone,
625 glyoxal, methylglyoxal, nonanal and decanal) in the atmosphere at Mt. Tai. Atmos.
626 Chem. Phys. 13, 5369-5380, doi:10.5194/acp-13-5369-2013.
627 Keene, W.C., Galloway, J.N., Holden Jr., J.D., 1983. Measurement of weak organic acidity in
628 precipitation from remote areas of the world. J. Geophys. Res. 88, 5122-5130.
629 Keene, W.C., Talbot, R.W., Andreae, M.O., Beecher, K., Berresheim, H., Castro, M., Farmer,
630 J.C., Galloway, J.N., Hoffmann, M.R., Li, S.M., Maben, J.R., Munger, J.W., Norton,
631 R.B., Pszenny, A.A.P., Puxbaum, H., Westberg, H., Winiwarter, W., 1989. An
632 intercomparison of measurement systems for vapor and particulate phase concentrations
633 of formic and acetic acids. J. Geophys. Res. 94, 6457-6471.
634 Kesselmeier, J., Staudt, M., 1999. Biogenic volatile organic compounds (VOC): An overview
635 on emission, physiology, and ecology. J. Atmos. Chem. 33, 23-88.
636 Khan, J., Brimblecombe, P., Glegg, S.L., 1995. Solubilities of pyruvic acid and the lower
637 (C_1-C_6) carboxylic acids. Experimental determination of equilibrium vapour pressures
638 above pure aqueous and salt solutions. J. Atmos. Chem. 22, 285-302.
639 Khwaja, H.A., 1995. Atmospheric concentrations of carboxylic acids and related compounds
640 at a semiurban site. Atmos. Environ. 29, 127-139.
641 Kudo, S., Tanimoto, H., Inomata, S., Saito, S., Pan, X., Kanaya, Y., Taketani, F., Wang, Z.,
642 Chen, H., Dong, H., Zhang, M., Yamaji, K., 2014. Emissions of non-methane volatile

643 organic compounds from open crop residue burning in the Yangtze River Delta region,
644 China. J. Geophys. Res. Atmos. 119, 7684-7698, doi:10.1002/2013JD021044.
645 Legrand, M., Gros, V., Preunlert, S., Estève, R.S., Thierry, A.M., Pèpy, G., Jourdain, B.,
646 2012. A reassessment of the budget of formic and acetic acids in the boundary layer at
647 Dumont d'Urville (coastal Antarctica): The role of penguin emissions on the budget of
648 several oxygenated volatile organic compounds. J. Geophys. Res. 117, D06308,
649 doi:10.1029/2011JD017012.
650 Li, S.M., Winchester, J.W., 1989. Geochemistry of organic and inorganic ions of late winter
651 arctic aerosols. Atmos. Environ. 33(11), 2401-2415.
652 Lim, H.J., Carlton, A.G., Turpin, B.J., 2005. Isoprene forms secondary organic aerosol
653 through cloud processing: model simulations. Environ. Sci. Technol. 39, 4441-4446.
654 Liu, J., Zhang, Z., Parker, E.T., Veres, P.R., Toberts, J.M., de Gouw, J.A., Hayes, P.L.,
655 Jimenez, J.L., Murphy, J.G., Ellis, R.A., Huey, L.G., Weber R.J., 2012, On the
656 gas-particle partitioning of soluble organic aerosol in two urban atmospheres with
657 contrasting emissions: 2. Gas and particle phase formic acid. J. Geophys. Res. 117,
658 D00V21.
659 Miyazaki, Y., Aggarwal, S.G., Singh, K., Gupta, P.K., Kawamura, K., 2009. Dicarboxylic
660 acids and water-soluble organic carbon in aerosols in New Delhi, India, in winter:
661 Characteristics and formation processes. J. Geophys. Res. 114, D19206,
662 doi:10.1029/2009JD011790.
663 Miyazaki, Y., Sawano, M., Kawamura, K., 2014. Low-molecular-weight hydroxyacids in
664 marine atmospheric aerosol: evidence of a marine microbial origin. Biogeosciences 11,
665 4407-4404.
666 Mochizuki, T., Kawamura, K., Aoki, K., Sugimoto, N., 2016. Long-range atmospheric
667 transport of volatile monocarboxylic acids with Asian dust over high mountain snow site,
668 central Japan. Atmos. Chem. Phys. 16, 14621-14633.

669 Möhler, O., Benz, S., Saathoff, H., Schnaiter, M., Wanger, R., Schneider, J., Walter, S., Ebert,
670 V., Wanger, S., 2008. The effect of organic coating on the heterogeneous ice nucleation
671 efficiency of mineral dust aerosols. Environ. Res. Lett. 3(2).
672 Nguyen, T.B., Bateman, A.P., Bones, D.L., Nizkorodov, S.A., Laskin, J., Laskin, A., 2010.
673 High-resolution mass spectrometry analysis of secondary organic aerosol generated by
674 ozonolysis of isoprene. Atmos. Environ. 44, 1032-1042.
675 Paciga, A.L., Riipinen, I., Pandis, S.N., 2014. Effect of ammonia on the volatility of organic
676 diacids. Environ. Sci. Technol. 48, 13769-13775.
677 Paulot, F., Wunch, D., Crounse, J.D., Toon, G.C., Millet, D.B., DeCarlo, P.F., Vigouroux, C.,
678 Deutscher, N.M., Abad, G.G., Notholt, J., Warneke, T., Hannigan, J.W., Warneke, C., de
679 Gouw, J.A., Dunlea, E.J., De Maziere, M., Griffith, D.W.T., Bernath, P., Jimenez, J.L.,
680 Wennberg, P.O., 2011. Importance of secondary sources in the atmospheric budgets of
681 formic and acetic acids. Atmos. Chem. Phys. 11, 1989-2013.
682 Pommier, M., Clerbaux, C., Coheur, P.F., Mahieu, E., Müller, J.F., Paton-Walsh, C.,
683 Stavrakou, T., Vigouroux, C., 2016. HCOOH distributions from IASI for 2008–2014:
684 comparison with ground-based FTIR measurements and a global chemistry-transport
685 model. Atmos. Chem. Phys. 16, 8963-8981.
686 Preunkert, S., Legrand, M., Jourdain, B., Dombrowski-Etchevers, I., 2007. Acidic gases
687 (HCOOH, CH_3COOH, HNO_3, HCl, and SO_2) and related aerosol species at a high
688 mountain Alpine site (4360 m elevation) in Europe. J. Geophys. Res. 112, D23S12,
689 doi:10.1029/2006JD008225.
690 Raja, S., Raghunathan, R., Yu, X.Y., Lee, T., Chen, J., Kommalapati, R.R., Murugesan, K.,
691 Shen, X., Qingzhong, Y., Valsaraj, K.T., Collett Jr., J.L., 2008. Fog chemistry in the
692 Texas-Louisiana Gulf Coast corridor. Atmos. Environ. 42, 2048-2061.

693 Rollins, A.W., Browne, E.C., Min, K.–E., Pusede, S.E., Wooldridge, P.J., Gentner, D.R.,
694 Goldstein, A.H., Liu, S., Day, D.A., Russell, L.M., Cohen, R.C., 2012. Evidence for NO_x
695 control over nighttime SOA formation. Science 337 (6099), 1210-1212.
696 Simoneit, B.R.T., 2002. Biomass burning – a review of organic tracers for smoke from
697 incomplete combustion. Appl. Geochem. 17, 129-162.
698 Stavrakou, T., Muller, J-F., Peeters, J., Razavi, A., Clarisse, L., Clerbaux, C., Coheur, P-F.,
699 Hurtmans, D., De Maziere, M., Vigouroux, C., Deutscher, N.M., Griffith, D.W.T., Jones,
700 N., Paton-Walsh, C., 2012. Satellite evidence for a large source of formic acid from
701 boreal and tropical forests. Nature Geoscience 5, 26-30.
702 Talbot, R.W., Beecher, K.M., Harriss, R.C., Cofer, W.R., 1988. Atmospheric geochemistry of
703 formic and acetic-acids at a mid-latitude temperate site. J. Geophys. Res. Atmos. 93,
704 1638-1652.
705 Tsai, Y.I., Kuo, S.C., 2013. Contributions of low molecular weight carboxylic acids to
706 aerosols and wet deposition in a natural subtropical broad-leaved forest environment
707 Atmos. Environ. 81, 270-279.
708 Wang, T., Cheung, T.F., Li, Y.S., Yu, X.M., Blake, D.R., 2002. Emission characteristics of
709 CO, NO_x, SO_2 and indications of biomass burning observed at a rural site in eastern
710 China. J. Geophys. Res. 107, 4157.
711 Wang, Y., Zhang, G., Tang, A., Yuan, H., Sun, Y., Chen, S., Zheng A., 2005. The ion
712 chemistry and the source of PM2.5 aerosol in Beijing. Atmos. Environ. 39, 3771-3784.
713 Wang, Y., Zhuang, G., Zhang, X., Huang, K., Xu, C., Tang, A., Chen, J., An, Z., 2006. The
714 ion chemistry, seasonal cycle, and sources of $PM_{2.5}$ and TSP aerosol in Shanghai. Atmos.
715 Environ. 40, 2935-2952.
716 Warneck, P., 2005. Multi-phase chemistry of C_2 and C_3 organic compounds in the marine
717 atmosphere. J. Atmos. Chem. 51, 119-159.

718 Yatavelli, R.L.N., Stark, H., Thompson, S.L., Kimmel, J.R., Cubison, M.J., Day, D.A.,
719 Campuzano-Jost, P., Palm, B.B., Hodzic, A., Thornton, J.A., Jayne, J.T., Eorsnop, D.R.,
720 Jimenez, J.L., 2014. Semicontinuous measurements of gas-particle partitioning of
721 organic acids in a ponderosa pine forest using a MOVI-HRToF-CIMS. Atmos. Chem.
722 Phys. 14, 1527-1546.
723 Yu, S., 2000. Role of organic acids (formic, acetic, pyruvic and oxalic) in the formation of
724 cloud condensation nuclei (CCN): a review. Atmos. Res. 53, 185-217.
725 Yuan, B., Veres, P.R., Warneke, C., Roberts, J.M., Gilman, J.B., Koss, A., Edwards, P.M.,
726 Graus, M., Kuster, W.C., Li, S.-M., Wild, R.J., Brown, S.S., Dubé, W.P., Lerner, B.M.,
727 Williams, E.J., Johnson, J.E., Quinn, P.K., Bates, T.S., Lefer, B., Hayes, P.L., Jimenez,
728 J.L., Weber, R.J., Zamora, R., Ervens, B., Millet, D.B., Rappenglück, B., de Gouw, J.A.,
729 2015. Investigation of secondary formation of formic acid: urban environment vs. oil and
730 gas producing region. Atmos. Chem. Phys. 15, 1975-1993.
731

Figure captions

Figure 1. A map of East Asia with the sampling site at Mt. Tai in the North China Plain.

Figure 2. Seven-day air mass back trajectories arriving at the summit of Mt. Tai (1534 m above sea level) at a level of 1500 m a. s. l. with fir spots in Central East China for selected periods in June 2006.

Figure 3. Temporal variations in the concentrations of major monocarboxylic acids in gas and particle phases and K^+. Open circles indicate gas phase samples and solid circles indicate particle phase samples. Shaded areas indicate nighttime.

Figure 4. Compositions of monocarboxylic acids in gas and particle phases during less field burning (LFB) and more field burning (LFB) influenced periods.

Figure 5. Temporal variations in particle phase fraction (F_p) for major organic acids. Shaded areas indicate nighttime.

Figure 6. Correlations of formic and acetic acids in gas and particle phases with levoglucosan in daytime during less field burning (LFB) and more field burning (LFB) influenced periods.

Figure 7. Correlations of formic and acetic acids in gas and particle phases with K^+ in daytime during less field burning (LFB) and more field burning (LFB) influenced periods.

Figure 8. Correlation plots of formic and acetic acids in gas and particle phases and carbon monoxide (CO) during less field burning (LFB) and more field burning (LFB) influenced periods.

Figure 9. Changes of contribution of particulate and gaseous acetic acid (C_2) to total monocarboxylic acids (total MCA) in the Mt Tai during less field burning (LFB) and more field burning (LFB) influenced periods.

Figure 10. Correlation plots of lactic acid and isopentanoic acid in gas and particle phases.

757

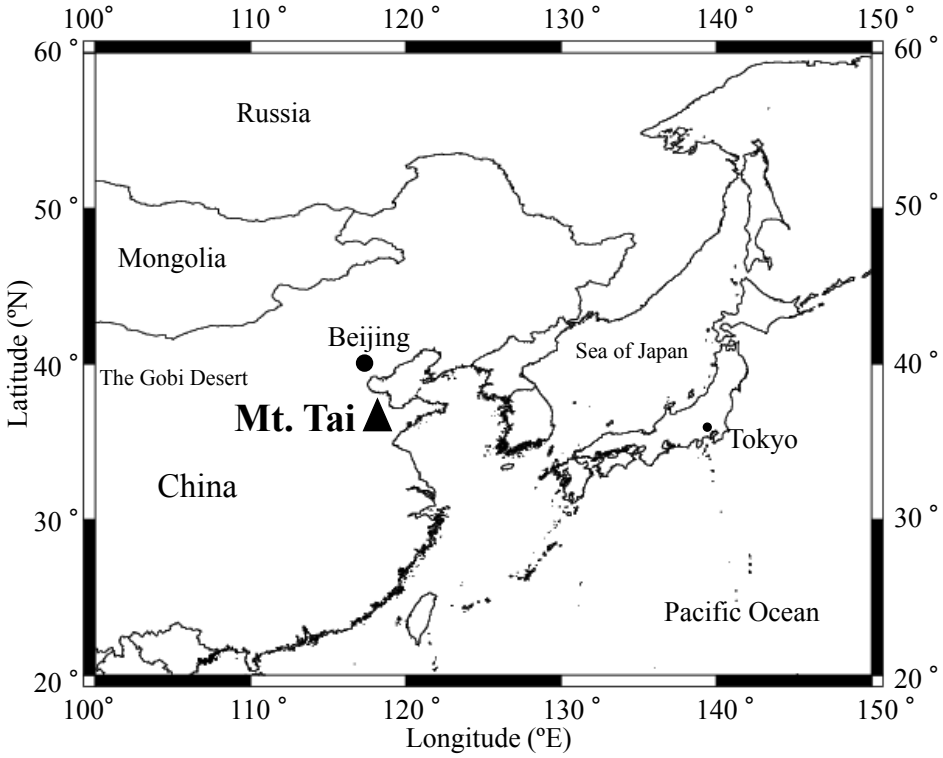

758

759 Figure 1. A map of East Asia with the sampling site at Mt. Tai in the North China Plain.

760

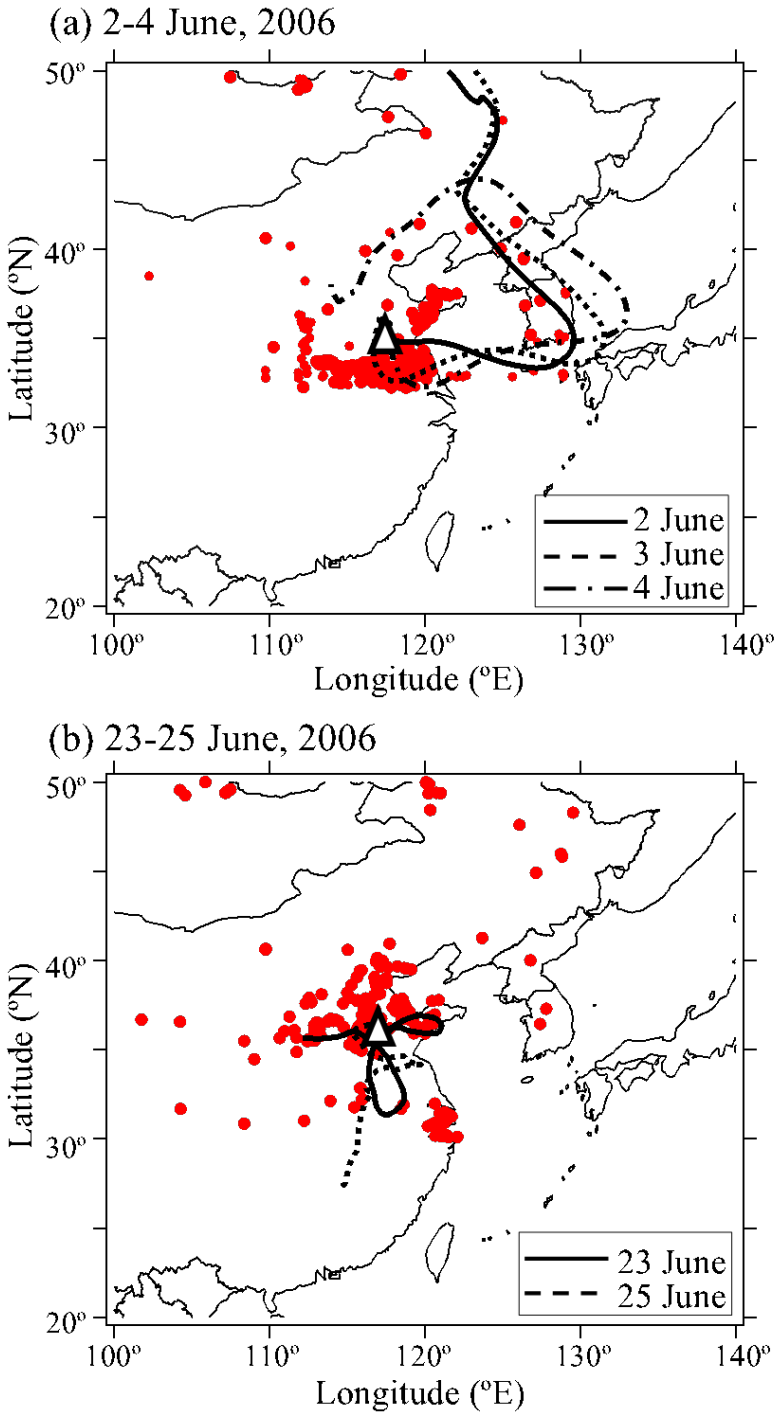

761

762 Figure 2. Seven-day air mass back trajectories arriving at the summit of Mt. Tai (1534 m
763 above sea level) at a level of 1500 m a. s. l. with fire spots in Central East China for selected
764 periods in June 2006.

765

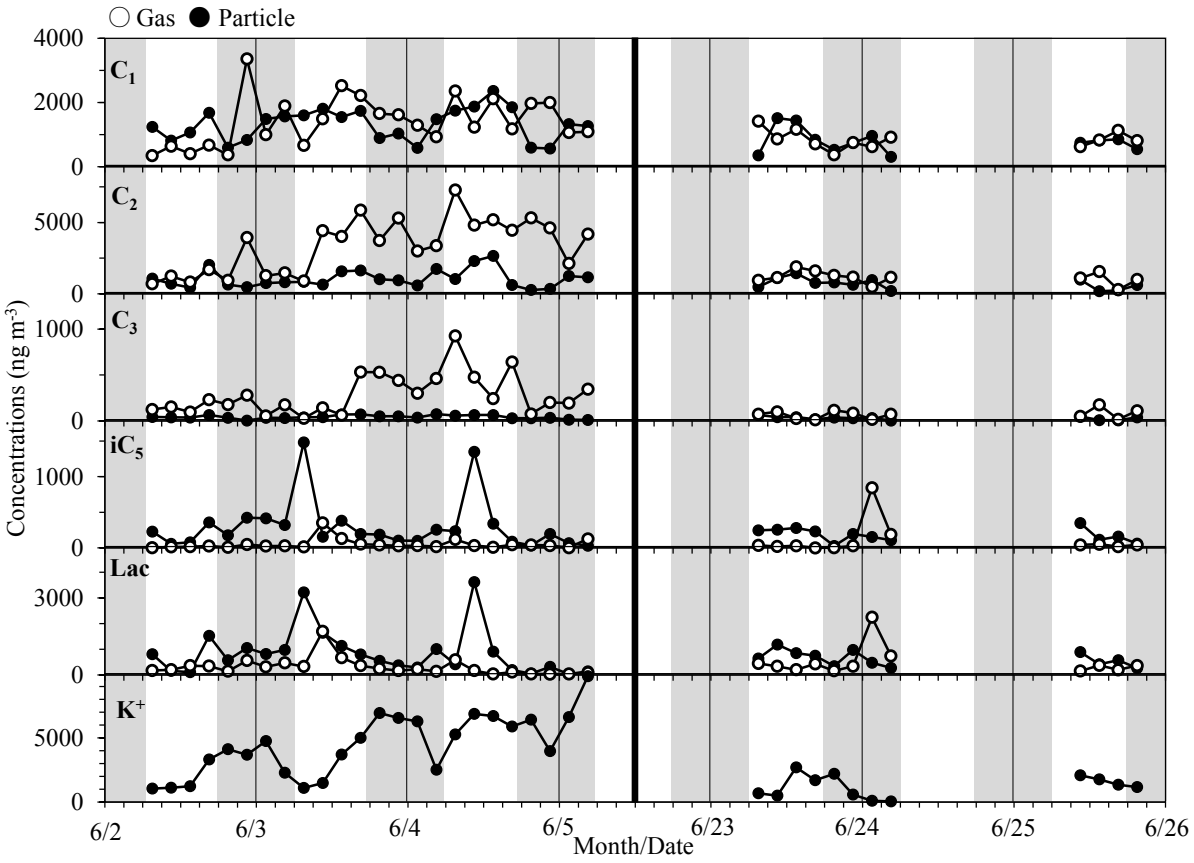

766

767 Figure 3. Temporal variations in the concentrations of major monocarboxylic acids in gas and

768 particle phases and K^+. Open circles indicate gas phase samples and solid circles indicate

769 particle phase samples. Shaded areas indicate nighttime.

770

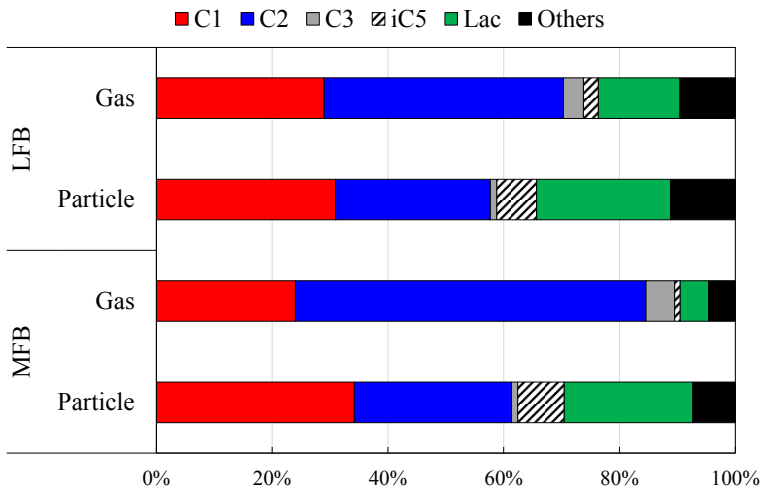

771

772 Figure 4. Compositions of monocarboxylic acids in gas and particle phases during less field

773 burning (LFB) and more field burning (LFB) influenced periods.

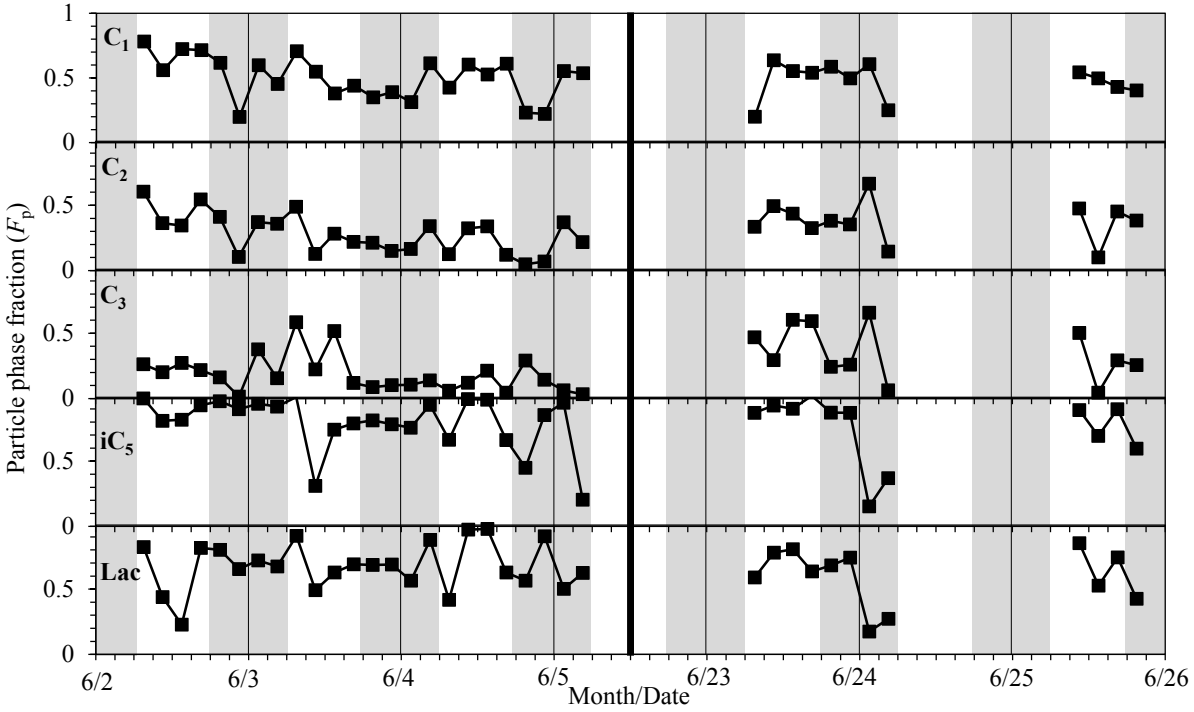

774

775 Figure 5. Temporal variations in particle phase fraction (F_p) for major organic acids. Shaded

776 areas indicate nighttime.

777

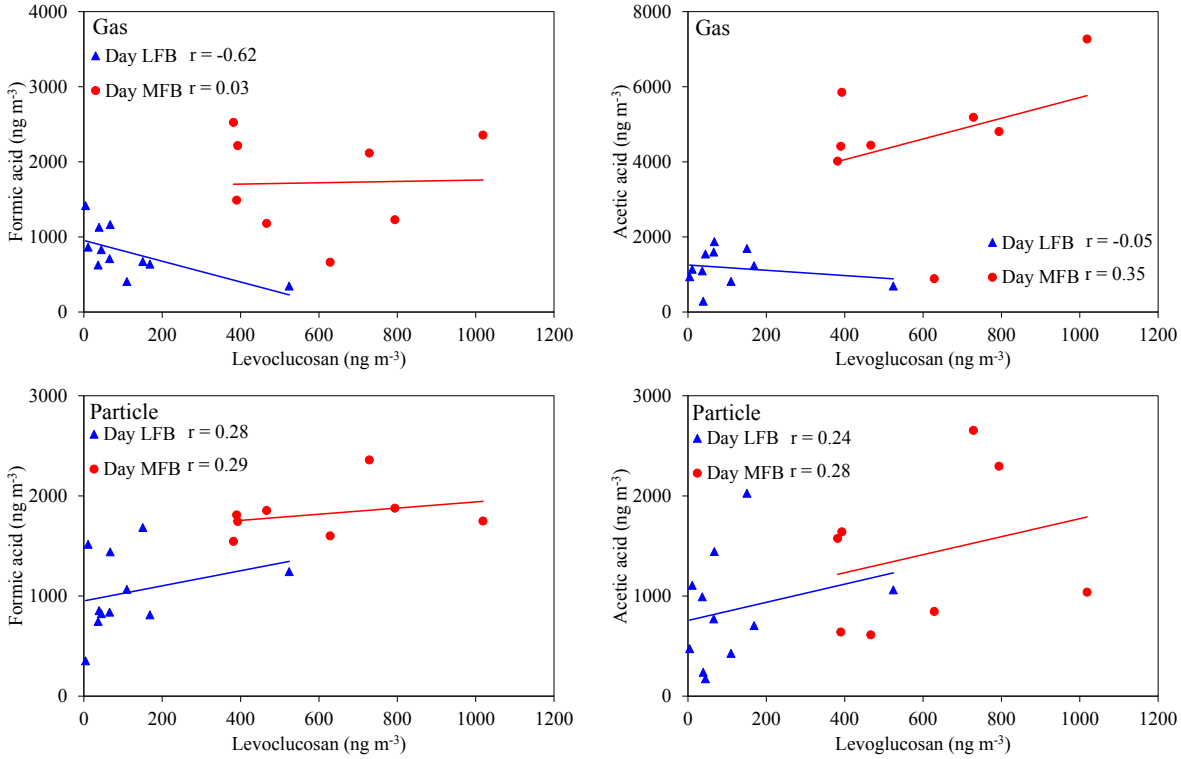

778

779

780 Figure 6. Correlations of formic and acetic acids in gas and particle phases with levoglucosan

781 in daytime during less field burning (LFB) and more field burning (LFB) influenced periods.

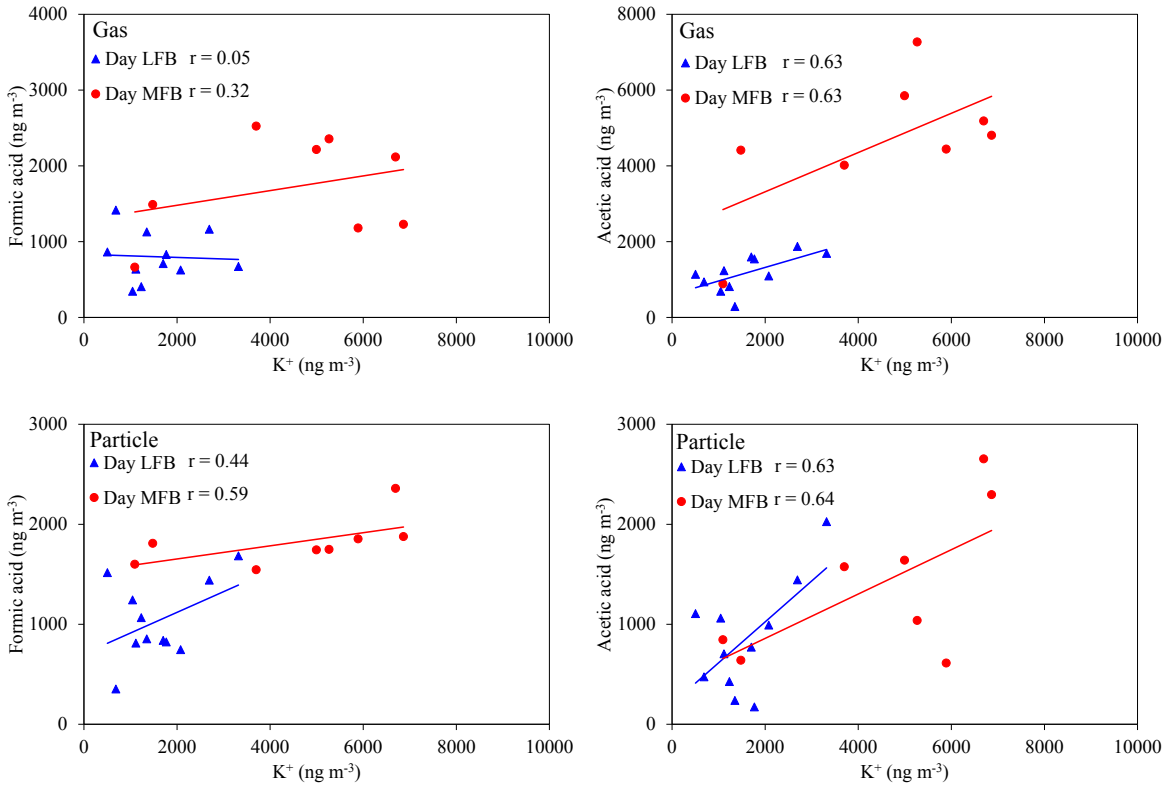

782

783

784 Figure 7. Correlations of formic and acetic acids in gas and particle phases with K^+ in

785 daytime during less field burning (LFB) and more field burning (LFB) influenced periods.

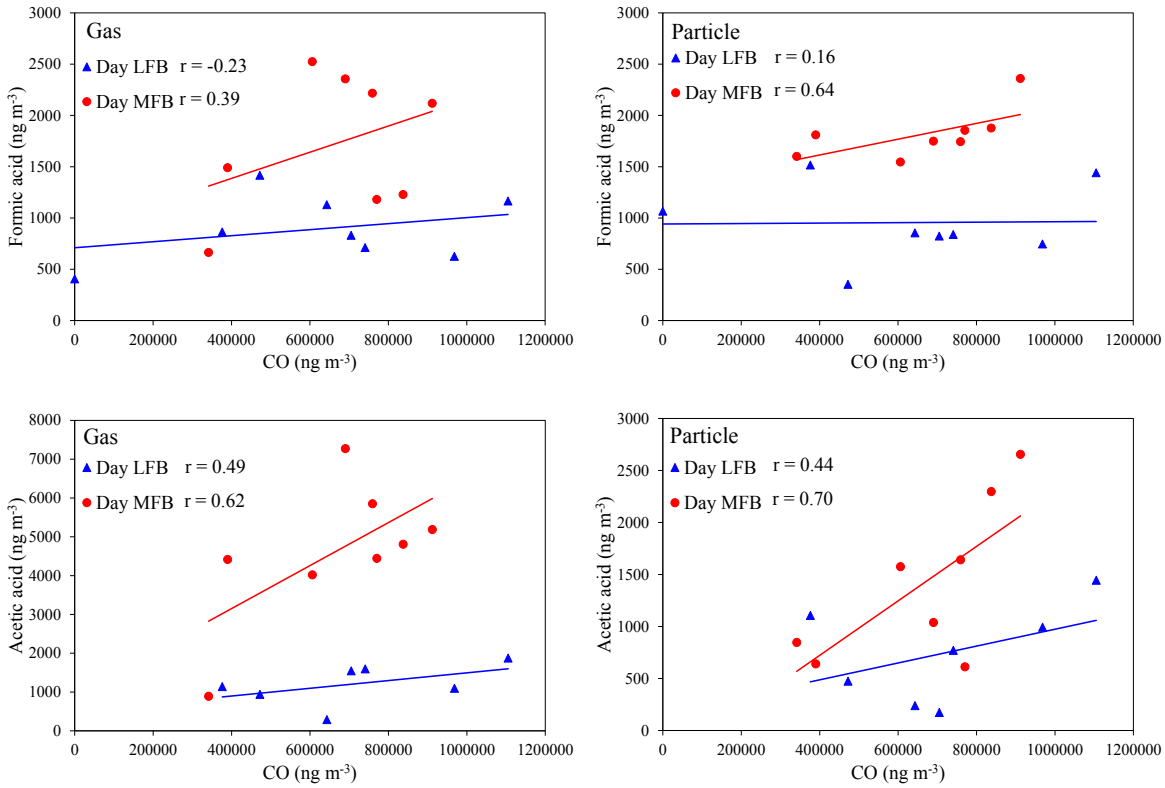

786

787

788 Figure 8. Correlation plots of formic and acetic acids in gas and particle phases and carbon

789 monoxide (CO) during less field burning (LFB) and more field burning (LFB) influenced

790 periods.

791

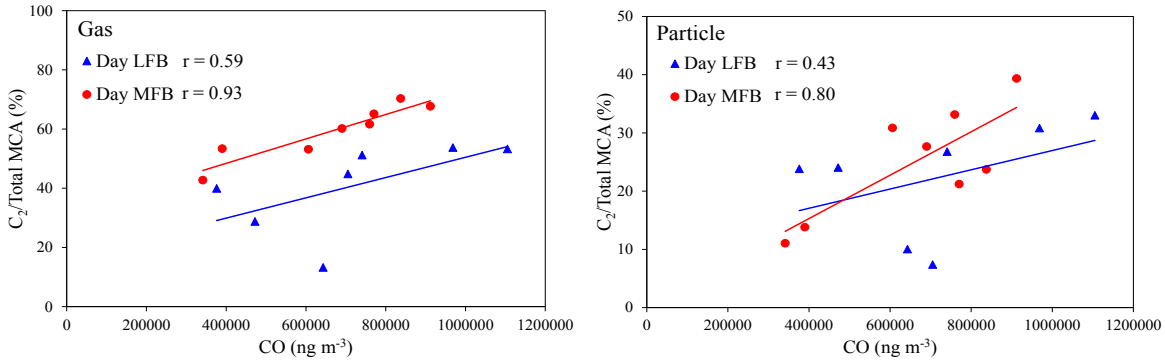

792

793 Figure 9. Changes of contribution of particulate and gaseous acetic acid (C_2) to total
794 monocarboxylic acids (total MCA) in the Mt Tai during less field burning (LFB) and more
795 field burning (LFB) influenced periods.

796

797

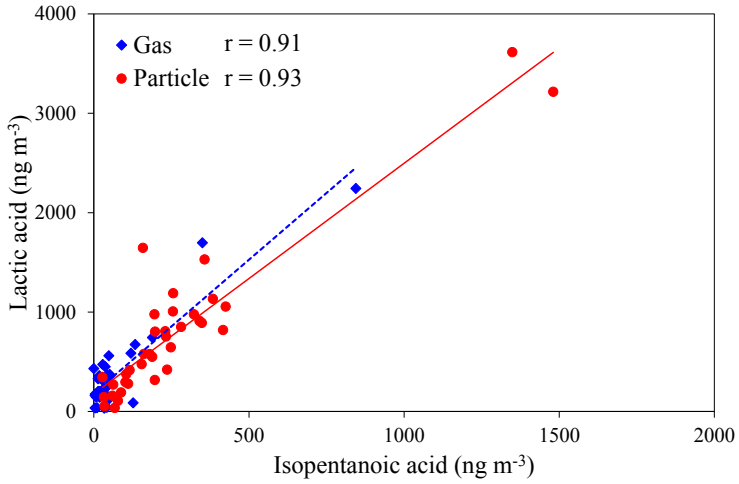

798

799 Figure 10. Correlation plots of lactic acid and isopentanoic acid in gas and particle phases.

Table 1. Average concentrations (ng m^{-3}) of gaseous and particulate low molecular weight monocarboxylic acids and particle phase fraction (F_p) during less field burning (LFB) and more field burning (MFB) influenced periods.

Acid species	MFB						LFB						MFB	LFB
	Gas			Particle			Gas			Particle			F_p	F_p
	min.	max.	average	min.	max.	average	min.	max.	average	min.	max.	average	average	average
Aliphatic acids														
Formic, C_1	664	2520	1570	570	2360	1410	346	3360	890	307	1690	883	0.47	0.52
Acetic, C_2	888	7270	3960	263	2650	1120	289	3940	1270	174	2030	763	0.24	0.38
Propionic, C_3	28	927	324	12	74	45	12	280	106	4	65	33	0.19	0.30
Isobutyric, iC_4	2	90	37	0	42	16	7	45	23	1	33	12	0.35	0.32
Butyric, C_4	4	192	77	3	42	17	5	83	36	1	26	11	0.30	0.27
Isopentanoic, iC_5	4	350	64	33	1480	331	0	844	79	28	425	196	0.76	0.80
Pentanoic, C_5	0	12	4	0	8	2	0	9	2	0	11	3	0.46	0.58
Isohexanoic, iC_6	0	8	2	0	4	2	0	4	0	0	5	2	0.62	0.92
Hexanoic, C_6	0	31	4	2	17	9	0	30	5	0	17	5	0.78	0.61
Heptanoic, C_7	0	5	2	0	10	2	0	5	2	1	7	2	0.48	0.50
Octanoic, C_8	0	10	3	1	41	13	0	15	8	1	26	11	0.77	0.57
Nonanoic, C_9	4	370	59	1	117	40	0	400	123	4	693	112	0.42	0.41
Decanoic, C_{10}	0	9	2	0	18	5	0	9	3	0	20	4	0.59	0.36
Sub total			6110			3010			2550			2040		
Aromatic acid														
Benzoic, Benz	2	119	40	5	98	27	6	48	25	2	34	17	0.51	0.39
Hydroxyacids														
Lactic, Lac	33	1700	319	36	3615	917	144	2240	433	107	1530	661	0.69	0.61
Glycolic, Glyco	12	343	72.1	14	348	168	16	125	65.1	25	431	140	0.71	0.65
Sub total			391			1090			498			801		

Table 2. Comparisons of atmospheric concentrations of formic and acetic acids in the atmosphere over Mt. Tai (this work) with those in previous studies from multiple sites in the world.

Location		Formic acid (ng m^{-3})	Acetic acid (ng m^{-3})	References
Mt. Tai, China (wheat biomass burning)	G	1570	3960	This study
Los Angeles (urban)	G	860	1800	Kawamura et al. (2000)
California, Pasadena (urban)	G	4000	—	Yuan et al. (2015)
Utah (oil and gas producing region)	G	4700	—	Yuan et al. (2015)
Amazon (tropical forest)	G	3400	5900	Andreae et al. (1988)
Yangtze River Delta region, China (biomass burning)	G	—	5000	Kudo et al. (2014)
Greenland (mountain)	G	1070	1070	Dibb and Arsenault (2002)
France (Alps)	G	640	750	Preunkert et al. (2007)
Pacific Ocean	G	55	122	Miyazaki et al. (2014)
Antarctica	G	92	75	Legrand et al. (2012)
Mt. Tai, China (wheat biomass burning)	P	1410	1120	This study
Los Angeles (urban)	P	163	120	Kawamura et al. (2000)
Amazon (tropical forest)	P	46	48	Andreae et al. (1988)
Pacific Ocean	P	2	8	Miyazaki et al. (2014)
Taiwan (subtropical forest)	P	30	312	Tsai and Kuo (2013)
Alaska	P	244	744	Li and Winchester (1989)
Beiging, China (urban)	P	370	350	Wang et al. (2005)
Shanghai, China (urban)	P	80	150	Wang et al. (2006)

G: gas-phase, P: particle-phase